CRLB for Estimation of 3D Sensor Biases in Spherical Coordinates and Its Attainability

MICHAEL KOWALSKI
DJEDJIGA BELFADEL
YAAKOV BAR-SHALOM
PETER WILLETT

In order to carry out data fusion, it is crucial to account for the imprecision of sensor measurements due to systematic errors. This requires estimation of the sensor measurement biases. In this paper, we consider a three-dimensional multisensor–multitarget maximum likelihood bias estimation approach for both additive and multiplicative biases in the measurements. Multiplicative biases can more accurately represent real biases in many sensors; however, they increase the complexity of the estimation problem. By converting biased measurements into pseudo-measurements of the biases, it is possible to estimate biases separately from target state estimation. The conversion of the spherical measurements to Cartesian measurements, which has to be done using the unbiased conversion, is the key that allows estimation of the sensor biases without having to estimate the states of the targets of opportunity. The measurements provided by these sensors are assumed time-coincident (synchronous) and perfectly associated. We evaluate the Cramér–Rao lower bound on the covariance of the bias estimates, which serves as a quantification of the available information about the biases. Through the use of the iterated least squares, it is proved that it is possible to achieve statistically efficient estimates.

Manuscript received January 18, 2019; revised April 9, 2019; released for publication July 8, 2019. Approved for Public Release 17-MDA-9446 (Dec. 15, 2017). There are no conflict of interest or financial disclosure statements relevant to this publication.

M. Kowalski, Y. Bar-Shalom, and P. Willett are with the Department of Electrical and Computer Engineering, University of Connecticut, Storrs, CT, USA
D. Belfadel is with the Department of Electrical Engineering, Fairfield University, Fairfield, CT, USA
E-mail: michael.p.kowalski@uconn.edu, dbelfadel@fairfield.edu, yaakov.bar-shalom@uconn.edu, peter.willett@uconn.edu

1557-6418/19/$17.00

I. INTRODUCTION

Bias estimation and compensation are essential steps in distributed tracking systems. The objective of sensor registration is to estimate the biases in sensor measurements, such as scale (multiplicative) and offset (additive) biases in range, azimuth, and elevation measurements, clock bias, and/or uncertainties in sensor positions [4]. Owing to this, much effort has been devoted in the last few years to bias estimation procedures for multisensor–multitarget tracking systems. Biases in sensors have been approximated in several ways, including error in sensor pointing and additive biases in the measurements. However, real sensor biases can be more complex than such approximations. One reason is a combination of both multiplicative and additive biases in measurements. That is, a bias may cause increased error in a target that is further away from the sensor or on the periphery of the sensor's field of view.

In [19] and [20], a joint track-to-track bias estimation and fusion approach based on equivalent measurements of the local tracks was proposed. In [14], an approach is used to carry out track-to-track association by assuming additive biases in 2D Cartesian coordinates. In [11], another approach based on pseudo-measurements along with expectation–maximization (EM) to perform joint fusion and registration was proposed. A different method that uses a multistart local search to handle the joint track-to-track association and bias estimation problem was introduced in [21]. The concept of pseudo-measurement was used in [15] for exact bias estimation with further extensions in [16] and [17]. In addition, these methods require perfect knowledge about each local filter and its dynamic model. Also, as the number of sensors increases, the bias estimation problem suffers from the curse of dimensionality because of the commonly used stacked bias vector implementation [10]. In [5], [7], and [9], pseudo-measurements are used with maximum likelihood (ML) to estimate a combination of rotational biases, position biases, and additive measurement biases in addition to presenting the hybrid Cramér–Rao lower bound (HCRLB) as a metric for evaluating estimator efficiency. This is expanded upon in [6] and [8] with EM methods used instead of ML.

In this paper, the novelty is to use the method and Cramér–Rao lower bound (CRLB) derived in [13] combined with an ML method using iterated least squares (ILS) to solve the problem of estimating both multiplicative and additive biases for three-dimensional (3D) spherical sensors. The primary novelty of this work is to extend the work in [15]–[17] to 3D sensors including an unbiased conversion of the measurement covariance found in [18]. This work also builds on previous bias estimation research in [5], [7], and [9] by using a nonlinear weighted ML method to avoid the problems with biased estimates and lack of statistical efficiency. Additionally, multiplicative biases are used instead of the combination of rotational biases, position biases, and

additive measurement biases. The difficulty with this is that it increases the complexity of the bias estimation problem: now there are two sources of error in the measurement other than noise and the error from the multiplicative bias varies depending on the location of the target. More targets are required and it becomes necessary for the targets to be spaced such that the multiplicative bias can be differentiated from the additive bias. Therefore, an analysis of the CRLB is made to determine whether this method can achieve accuracy in bias estimates that is comparable to the error from noise. The CRLB gives a lower bound on the accuracy of bias estimates when using the pseudo-measurements, allowing analysis of performance when the measurement conversion is used rather than the raw measurements. Through the use of the pseudo-measurement model described in [15]–[17], it is possible to avoid the need to estimate the states of the targets and estimate only the sensor biases. Once the sensor biases are estimated, they can be removed from the measurements and the (nearly) bias-free measurements can then be used in tracking systems.

An important metric when using pseudo-measurements is the HCRLB that is discussed in [5], [7], and [9] and evaluated using ML methods. The HCRLB is the CRLB but calculated using all measurements and a parameter vector including the bias variables and all nuisance variables. In this case, the nuisance variables that are included are the target states. The removal of the target state in the calculation of the CRLB may result in a higher metric than the true lower bound that takes into account all the nuisance parameters available to the estimator. This means that it is necessary to include this metric in simulation results to understand how much accuracy is lost using the pseudo-measurement model. It is important to note that the HCRLB is a lower bound and may not be achieved by an estimator; however, EM approaches can be used to improve results such that they are closer to the HCRLB [6], [8]. Furthermore, estimating every nuisance variable may be computationally intensive, which would make the pseudo-measurement method attractive despite the loss of accuracy. Finally, calculating the CRLB does not require information about the target state, unlike the HCRLB that requires an estimate of the target states.

The paper is structured as follows. The bias model and the assumptions for bias estimation are discussed in Section II. In Section III, a review of the exact bias estimation method is given. The key to create the bias pseudo-measurements in Cartesian coordinates, which allows avoiding the need to estimate the states of the targets of opportunity, is to use the unbiased transformation from spherical to Cartesian [18]. The pseudo-measurement model is presented in Section III-A and the ILS estimator is described in Section III-B. Section III-C presents the calculation of the CRLB for the proposed method. Section IV demonstrates the performance of the method for synchronous sensors and compares the root mean squared error (RMSE) of the estimator with the CRLB. Conclusions are discussed in Section V.

II. PROBLEM FORMULATION

A. Coordinate Frames and Measurement Space

In a typical 3D sensor, the measured values of position are in spherical coordinates—range, azimuth, and elevation. Assume there are N_S synchronized sensors, with known positions, reporting range, azimuth, and elevation measurements in spherical coordinates of $t = 1, \ldots, N_T$ targets in the common surveillance region with K total time steps. The true range, azimuth, and elevation are represented by $r_{s,t}(k)$, $\theta_{s,t}(k)$, and $\alpha_{s,t}(k)$, respectively. The noise- and bias-free measurements originating from target t for sensor s at time k are

$$\begin{aligned} r_{s,t}(k) &= \sqrt{x_{s,t}(k)^2 + y_{s,t}(k)^2 + z_{s,t}(k)^2} \\ \theta_{s,t}(k) &= \tan^{-1}\left(\frac{y_{s,t}(k)}{x_{s,t}(k)}\right) \\ \alpha_{s,t}(k) &= \tan^{-1}\left(\frac{z_{s,t}(k)}{\sqrt{x_{s,t}(k)^2 + y_{s,t}(k)^2}}\right). \end{aligned} \tag{1}$$

Each sensor views the target using its own sensor reference frame; therefore,

$$\begin{aligned} \mathbf{x}_{s,t}(k) &= \begin{bmatrix} x_{s,t}(k) \\ y_{s,t}(k) \\ z_{s,t}(k) \end{bmatrix} = \begin{bmatrix} x_t(k) - x_s(k) \\ y_t(k) - y_s(k) \\ z_t(k) - z_s(k) \end{bmatrix} \\ &= \mathbf{x}_t(k) - \mathbf{x}_s(k) \end{aligned} \tag{2}$$

where $\mathbf{x}_t(k) = [x_t(k), y_t(k), z_t(k)]$ is the true position in Cartesian coordinates of target t at time step k and $\mathbf{x}_s(k) = [x_s(k), y_s(k), z_s(k)]$ is the true position in Cartesian coordinates of sensor s at time step k. Transforming (1) to a Cartesian coordinate frame yields

$$\begin{aligned} x^c_{s,t}(k) &= r_{s,t}(k)\cos\left(\theta_{s,t}(k)\right)\cos\left(\alpha_{s,t}(k)\right) \\ y^c_{s,t}(k) &= r_{s,t}(k)\sin\left(\theta_{s,t}(k)\right)\cos\left(\alpha_{s,t}(k)\right) \\ z^c_{s,t}(k) &= r_{s,t}(k)\sin\left(\alpha_{s,t}(k)\right). \end{aligned} \tag{3}$$

For a given sensor, each measurement is modeled as a function of the actual (true) target state, systematic errors (biases), and random errors (noise). The model for the measurements originating from a target with additive and multiplicative biases at time k in spherical coordinates for sensor s is

$$\begin{aligned} z_{s,t}(k) &= \begin{bmatrix} r^m_{s,t}(k) \\ \theta^m_{s,t}(k) \\ \alpha^m_{s,t}(k) \end{bmatrix} \\ &= \begin{bmatrix} \left[1 + \epsilon^r_s(k)\right] r_{s,t}(k) + b^r_s + w^r_s(k) \\ \left[1 + \epsilon^\theta_s(k)\right] \theta_{s,t}(k) + b^\theta_s + w^\theta_s(k) \\ \left[1 + \epsilon^\alpha_s(k)\right] \alpha_{s,t}(k) + b^\alpha_s + w^\alpha_s(k) \end{bmatrix} \\ & \qquad s = 1, \ldots, N_S, \quad t = 1, \ldots, N_T \end{aligned} \tag{4}$$

where $r^m_{s,t}(k)$, $\theta^m_{s,t}(k)$, and $\alpha^m_{s,t}(k)$ are the measured range, azimuth, and elevation, respectively, b^r_s, b^θ_s, and b^α_s are the offset biases in the range, azimuth, and elevation, respectively, and $\epsilon^r_s(k)$, $\epsilon^\theta_s(k)$, and $\epsilon^\alpha_s(k)$ are the scale biases in the range, azimuth, and elevation, respectively. The measurement noises $w^r_s(k)$, $w^\theta_s(k)$, and $w^\alpha_s(k)$ in range, azimuth, and elevation are zero mean with corresponding variances σ^2_r, σ^2_θ, and σ^2_α, respectively, and are assumed mutually independent. The bias vector for sensor s is

$$\beta_s = [\, b^r_s \quad b^\theta_s \quad b^\alpha_s \quad \epsilon^r_s \quad \epsilon^\theta_s \quad \epsilon^\alpha_s \,]^{\mathrm{T}} \tag{5}$$

and is modeled as an unknown constant over a certain window of scans (nonrandom variable). Consequently, the ML estimator [2] or the least-squares estimator [1] can be used for bias estimation. On the other hand, a Gauss–Markov random model [22] can also be used, in which case a Kalman filter can be adopted for bias estimation. We model the measurement equation (4) as

$$z_{s,t}(k) = \begin{bmatrix} r_{s,t}(k) \\ \theta_{s,t}(k) \\ \alpha_{s,t}(k) \end{bmatrix} + C_{s,t}(k)\beta_s + \begin{bmatrix} w^r_s(k) \\ w^\theta_s(k) \\ w^\alpha_s(k) \end{bmatrix} \tag{6}$$

where

$$C_{s,t}(k) \triangleq \begin{bmatrix} 1 & 0 & 0 & r_{s,t}(k) & 0 & 0 \\ 0 & 1 & 0 & 0 & \theta_{s,t}(k) & 0 \\ 0 & 0 & 1 & 0 & 0 & \alpha_{s,t}(k) \end{bmatrix}. \tag{7}$$

Here, the measured azimuth $\theta^m_{s,t}(k)$, elevation $\alpha^m_{s,t}(k)$, and range $r^m_{s,t}(k)$ can be utilized in (7) without any significant loss of performance [15]–[17].

The problem is to estimate the bias vectors β_s for all sensors. After bias estimation, all the biases can be compensated for to obtain the state estimates. Since the motion equations of targets are naturally expressed in Cartesian coordinates, if the spherical measurements can be converted to Cartesian (via nonlinear transformation) without introducing coordinate conversion bias and obtaining the correct covariance for the converted measurements, one can then perform the state estimation within a completely linear framework. Then, sensor s has the measurement equation in Cartesian coordinates (with the same $H_s(k) = H(k)$ for all sensors)

$$z^c_{s,t}(k) = H(k)\mathbf{x}_t(k) + B_{s,t}(k)C_{s,t}(k)\beta_s + \mathbf{x}_s(k) + w_s(k) \tag{8}$$

where the state vector is

$$\mathbf{x}_t(k) = \left[x_t(k)\ y_t(k)\ z_t(k)\right]^{\mathrm{T}} \tag{9}$$

and $H(k)$ is the measurement matrix given by

$$H(k) = \begin{bmatrix} 1 & 0 & 0 \\ 0 & 1 & 0 \\ 0 & 0 & 1 \end{bmatrix} \triangleq H. \tag{10}$$

Using the measured azimuth $\theta^m_{s,t}(k)$, elevation $\alpha^m_{s,t}(k)$, and range $r^m_{s,t}(k)$ from sensor s, the Jacobian of the Cartesian measurements with respect to the biases in each coordinate, $B_{s,t}(k)$, can be written (omitting subscripts s and t, superscript m, and time step k for simplicity) as

$$B_{s,t}(k) = \begin{bmatrix} \cos\theta\cos\alpha & -r\sin\theta\cos\alpha & -r\cos\theta\sin\alpha \\ \sin\theta\cos\alpha & r\cos\theta\cos\alpha & -r\sin\theta\sin\alpha \\ \sin\alpha & 0 & r\cos\alpha \end{bmatrix}. \tag{11}$$

The transformation of the measurements from spherical to Cartesian coordinates that has to be used is the unbiased one [18]. This was found necessary to ensure the accuracy of the bias estimates and is discussed in more detail at the end of the section.

The unbiased conversion converts the original measurements with the following equations:

$$\begin{aligned} x^{c,m}_{s,t}(k) &= \lambda^{-1}_\theta \lambda^{-1}_\alpha r_{s,t}(k)\cos\theta_{s,t}(k)\cos\alpha_{s,t}(k) + x_s(k) \\ y^{c,m}_{s,t}(k) &= \lambda^{-1}_\theta \lambda^{-1}_\alpha r_{s,t}(k)\sin\theta_{s,t}(k)\cos\alpha_{s,t}(k) + y_s(k) \\ z^{c,m}_{s,t}(k) &= \lambda^{-1}_\alpha r_{s,t}(k)\sin\alpha_{s,t}(k) + z_s(k) \end{aligned} \tag{12}$$

$$z^{c,m}_{s,t}(k) = \begin{bmatrix} x^{c,m}_{s,t}(k) \\ y^{c,m}_{s,t}(k) \\ z^{c,m}_{s,t}(k) \end{bmatrix}. \tag{13}$$

The new (unbiased) covariance matrix of the measurements in Cartesian coordinates (omitting indexes m and k in the measurements for simplicity) is given by

$$R_{s,t}(k) = \begin{pmatrix} R^{s,t}_{xx} & R^{s,t}_{xy} & R^{s,t}_{xz} \\ R^{s,t}_{xy} & R^{s,t}_{yy} & R^{s,t}_{yz} \\ R^{s,t}_{xz} & R^{s,t}_{yz} & R^{s,t}_{zz} \end{pmatrix} \tag{14}$$

$$\begin{aligned} R^{s,t}_{xx} &= (\lambda^{-2}_\theta \lambda^{-2}_\alpha - 2) r^2_{s,t}\cos^2\theta_{s,t}\cos^2\alpha_{s,t} \\ &\quad + \frac{1}{4}(r^2_{s,t} + \sigma^2_r)(1 + \lambda'_\theta \cos 2\theta_{s,t})(1 + \lambda'_\alpha \cos 2\alpha_{s,t}) \\ R^{s,t}_{yy} &= (\lambda^{-2}_\theta \lambda^{-2}_\alpha - 2) r^2_{s,t}\sin^2\theta_{s,t}\cos^2\alpha_{s,t} \\ &\quad + \frac{1}{4}(r^2_{s,t} + \sigma^2_r)(1 - \lambda'_\theta \cos 2\theta_{s,t})(1 + \lambda'_\alpha \cos 2\alpha_{s,t}) \\ R^{s,t}_{zz} &= (\lambda^{-2}_\alpha - 2) r^2_{s,t}\sin^2\alpha_{s,t} \\ &\quad + \frac{1}{2}(r^2_{s,t} + \sigma^2_r)(1 - \lambda'_\alpha \cos 2\alpha_{s,t}) \\ R^{s,t}_{xy} &= (\lambda^{-2}_\theta \lambda^{-2}_\alpha - 2) r^2_{s,t}\sin\theta_{s,t}\cos\theta_{s,t}\cos^2\alpha_{s,t} \\ &\quad + \frac{1}{4}(r^2_{s,t} + \sigma^2_r)\lambda'_\theta \sin 2\theta_{s,t}(1 + \lambda'_\alpha \cos 2\alpha_{s,t}) \\ R^{s,t}_{xz} &= (\lambda^{-1}_\theta \lambda^{-2}_\alpha - \lambda^{-1}_\theta - \lambda_\theta) r^2_{s,t}\cos\theta_{s,t}\sin\alpha_{s,t}\cos\alpha_{s,t} v \\ &\quad + \frac{1}{2}(r^2_{s,t} + \sigma^2_r)\lambda_\theta \lambda'_\alpha \cos\theta_{s,t}\sin 2\alpha_{s,t} \\ R^{s,t}_{yz} &= (\lambda^{-1}_\theta \lambda^{-2}_\alpha - \lambda^{-1}_\theta - \lambda_\theta) r^2_{s,t}\sin\theta_{s,t}\sin\alpha_{s,t}\cos\alpha_{s,t} \\ &\quad + \frac{1}{2}(r^2_{s,t} + \sigma^2_r)\lambda_\theta \lambda'_\alpha \sin\theta_{s,t}\sin 2\alpha_{s,t} \end{aligned} \tag{15}$$

where

$$\lambda_\theta = e^{-\sigma_\theta^2/2}$$
$$\lambda'_\theta = e^{-2\sigma_\theta^2} = \lambda_\theta^4$$
$$\lambda_\alpha = e^{-\sigma_\alpha^2/2}$$
$$\lambda'_\alpha = e^{-2\sigma_\alpha^2} = \lambda_\alpha^4. \tag{16}$$

The debiasing coefficients (16) are used in the calculation of the converted covariance matrix and this conversion bias interferes with the estimation of the consistent measurement biases. If the debiasing coefficients are zero, then the converted covariance matrix results in negative values, which causes negative values in the CRLB. Furthermore, the conversion bias adds to the error resulting from the measurement biases. The estimator has difficulty in differentiating this error from the error from the biases. If there is no noise or extremely little noise, it is possible to use the standard conversion to estimate the biases, but without CRLB efficiency. This is unreliable though and results may vary depending on the number of targets, their positions, and the magnitude of the biases, and in any case, the unbiased conversion adds little numerical complication.

Additionally, the calculation of the covariance matrix is necessary for use in ML methods in order to avoid biased estimates and to generate the CRLB. If a least-squares method is used but with identity noise rather than an accurate measurement noise matrix, it is likely to result in statistically inefficient estimates and potentially biased estimates [5], [7], [9].

III. SYNCHRONOUS SENSOR REGISTRATION FOR THE 3D CASE

In this section, the bias estimation method introduced in [15]–[17] for synchronous sensors with known sensor locations is reviewed and extended to the 3D case, with various simulations and the calculation of the lower bounds for bias estimation in multisensor–multitarget scenarios.

The estimator uses a batch of measurements from a number of time steps to estimate the biases. The parameter vector to be estimated consists of the biases, and pseudo-measurements are used to measure the effect of the biases. The pseudo-measurements remove the true target states in order to only measure the effect of the biases. The target states are not estimated with this estimator.

The dynamic equation for the target state is

$$\mathbf{x}(k) = \left[\mathbf{x}_t(k)^{\mathrm{T}}, \dot{\mathbf{x}}_t(k)^{\mathrm{T}}, \ddot{\mathbf{x}}_t(k)^{\mathrm{T}}\right]^{\mathrm{T}} \tag{17}$$

$$\mathbf{x}(k+1) = F(k)\mathbf{x}(k) + \mathbf{v}(k) \tag{18}$$

where $F(k)$ is the transition matrix and $\mathbf{v}(k)$ is a zero-mean additive white Gaussian noise with covariance $Q(k)$.

Because the local trackers are not able to estimate the biases on their own, they yield inaccurate estimates of tracks by assuming no bias in their measurements. Hence, the state space model considered by local trackers for a specific target t and sensor s is

$$\mathbf{x}_t(k+1) = \mathbf{x}_t(k) + F_t(k)\left[\dot{\mathbf{x}}_t(k)^{\mathrm{T}}\ddot{\mathbf{x}}_t(k)^{\mathrm{T}}\right]^{\mathrm{T}} + v(k) \tag{19}$$

$$z_{s,t}(k) = H(k)\mathbf{x}_t(k) + w_s(k) \tag{20}$$

where $F_t(k)$ is a submatrix of $F(k)$. In this method, the transition matrix can be unknown as the target state is not estimated. The difference between (4) and (20) is that the latter has no bias term and, as a result, the local tracks are bias-ignorant [15]–[17]. Note that this mismatch should be compensated for.

A. The Pseudo-Measurement of the Bias Vector

In this subsection, a discussion on how to find an informative pseudo-measurement by using the local tracks for the case $N_S = 2$ synchronized 3D sensors is presented, generalizing the method given in [15]–[17].

The pseudo-measurement of the bias vector is defined as

$$z_t^p(k) \triangleq z_{1,t}^c(k) - z_{2,t}^c(k) \tag{21}$$

In the above equation, the true position of the target is eliminated because of cancellation since each such position is multiplied by the same matrix (24). This results in the following equation:

$$z_t^p(k) = B_{1,t}(k)C_{1,t}(k)\beta_1 - B_{2,t}(k)C_{2,t}(k)\beta_2 + w_1(k) - w_2(k). \tag{22}$$

The pseudo-measurement of the bias vector can be written as

$$z_t^p(k) = \mathcal{H}_t(k)\mathbf{b} + \tilde{w}(k) \tag{23}$$

where the pseudo-measurement matrix $\mathcal{H}$, the bias parameter vector $\mathbf{b}$, and the pseudo-measurement noise $\tilde{w}(k)$ are defined as

$$\mathcal{H}_t(k) \triangleq \begin{bmatrix} (B_{1,t}(k)C_{1,t}(k))^{\mathrm{T}} \\ (-B_{2,t}(k)C_{2,t}(k))^{\mathrm{T}} \end{bmatrix}^{\mathrm{T}} \tag{24}$$

$$\mathbf{b} \triangleq \left[\beta_1^{\mathrm{T}}, \beta_2^{\mathrm{T}}\right]^{\mathrm{T}} \tag{25}$$

and

$$\tilde{w}(k) \triangleq w_1(k) - w_2(k). \tag{26}$$

The bias pseudo-measurement noises $\tilde{w}$ are additive white Gaussian with zero mean, and their covariance is

$$\mathcal{R}_t(k) = R_{1,t}(k) + R_{2,t}(k). \tag{27}$$

The key property of (26) is its whiteness, which results in an exact bias estimate. In this approach, there is no

approximation in deriving (23)–(27) unlike the methods previously proposed in [12], [23], and [24]. This was one of the main contributions of [15].

B. The ILS Method

If the biases are constant for each measurement over the batch of scans, then an ILS method can be used. This estimator finds the ML estimate [3] of the bias vector $\mathbf{b}$. This estimator uses the Jacobian calculated previously in (24) for the pseudo-measurements of the bias vector as well as the noise covariance matrix (27). The measurements and matrices must be stacked in a batch for the estimator. The measurement batch is

$$\mathbf{z}^p = \left[z_1^p(1)^{\mathrm{T}}, \ldots, z_1^p(K)^{\mathrm{T}}, z_2^p(1)^{\mathrm{T}}, \ldots, z_{N_T}^p(K)^{\mathrm{T}}\right]^{\mathrm{T}}. \quad (28)$$

The Jacobian matrix batch is defined for each estimator iteration j as

$$\mathbf{H}^j = [\mathcal{H}_1^j(1)^{\mathrm{T}}, \ldots, \mathcal{H}_1^j(K)^{\mathrm{T}}, \mathcal{H}_2^j(1)^{\mathrm{T}}, \ldots, \mathcal{H}_{N_T}^j(K)^{\mathrm{T}}]^{\mathrm{T}}. \quad (29)$$

The noise covariance for the batch is a diagonal matrix composed of the individual covariance matrices

$$\mathbf{R} = \begin{bmatrix} \mathcal{R}_1(1) & 0 & 0 & 0 & 0 \\ 0 & \ldots & 0 & 0 & 0 \\ 0 & 0 & \mathcal{R}_1(K) & 0 & 0 \\ 0 & 0 & 0 & \ldots & 0 \\ 0 & 0 & 0 & 0 & \mathcal{R}_{N_T}(K) \end{bmatrix}. \quad (30)$$

The equation for each iteration j of the estimator is

$$\mathbf{b}_e^{j+1} = \mathbf{b}_e^j + [\mathbf{H}^{j\mathrm{T}}\mathbf{R}^{-1}\mathbf{H}^j]^{-1}\mathbf{H}^{j\mathrm{T}}\mathbf{R}^{-1}[\mathbf{z}^p - \mathbf{h}(\mathbf{b}_e^j)]. \quad (31)$$

At each iteration, the current state estimate is used to generate a predicted measurement vector to compare to the actual measurements

$$\mathbf{h}(\mathbf{b}_e^j) = \mathbf{H}^j\mathbf{b}_e^j. \quad (32)$$

When the state no longer changes significantly, then the estimator stops and takes the final iteration as its estimated parameter. To initialize the estimator, the biases are assumed to be zero

$$\mathbf{b}_e^0 = [0, 0, \ldots, 0]^{\mathrm{T}}. \quad (33)$$

In order for the estimator to be observable, a bare minimum of measurements is needed to satisfy the requirement that there will be at least one pseudo-measurement per parameter vector element. This results in the following inequality:

$$3KN_T\,(N_S - 1) \geq 6N_S. \quad (34)$$

This inequality can be simplified to

$$KN_T - \frac{KN_T}{N_S} \geq 2. \quad (35)$$

In practice, more measurements than this are required together with measurement diversity to obtain satisfactory accuracy. In order to have sufficient measurement diversity, there must be targets spaced such that for one target the error from the multiplicative bias is larger than the error from the additive bias and for another target the error from the additive bias is larger than the error from the multiplicative bias.

C. CRLB for the Biases

To investigate the performance of the estimator, it is necessary to calculate the CRLB. The CRLB is defined [3] as the inverse of the Fisher information matrix.

$$\mathrm{CRLB} = \mathbf{J}^{-1} = [\mathbf{H}^{\mathrm{T}}\mathbf{R}^{-1}\mathbf{H}]^{-1}. \quad (36)$$

The CRLB is based on the batch of Jacobians that is calculated in (29) and (24) as well as the batch of noise covariance matrices calculated in (30), (27), and (14). The calculation of the CRLB does not require any knowledge of the target state, although the spherical measurements are used in calculating (11) and (7). It will be shown in the next section that the covariance of the bias estimates attains the CRLB; i.e., the ML estimator is efficient for this problem.

We additionally calculate the HCRLB that is a more accurate lower bound as some of the information in the 3D spherical measurements has been eliminated to produce the pseudo-measurements. The HCRLB takes into account the nuisance variables not originally estimated, in this case the target positions. The parameter vector for the HCRLB is

$$\psi = \left[\mathbf{b}^{\mathrm{T}}, \mathbf{x}_{t1}(1), \ldots, \mathbf{x}_{t1}(K), \ldots, \mathbf{x}_{N_t}(K)\right]^{\mathrm{T}}. \quad (37)$$

The HCRLB is defined as

$$\mathrm{HCRLB} = [\mathbf{H}_\psi^{\mathrm{T}}\mathbf{R}_\psi^{-1}\mathbf{H}_\psi]^{-1} \quad (38)$$

where the Jacobian and covariance associated with the HCRLB are defined as

$$\begin{aligned} \mathbf{H}_\psi &= \nabla_\psi \mathbf{z} \\ &= \nabla_\psi \left[z_{s1,t1}(1)^{\mathrm{T}}, \ldots, z_{s1,t1}(K)^{\mathrm{T}}, \ldots, z_{N_s,N_t}(K)^{\mathrm{T}}\right]^{\mathrm{T}} \end{aligned} \quad (39)$$

$$\mathbf{R}_\psi = \begin{bmatrix} \sigma_r^2 & 0 & 0 & \ldots \\ 0 & \sigma_\alpha^2 & 0 & \ldots \\ 0 & 0 & \sigma_\epsilon^2 & \ldots \\ \ldots & \ldots & \ldots & \ldots \end{bmatrix}. \quad (40)$$

For brevity, the individual derivatives are not included. The HCRLB is calculated using the true values of the biases and target states.

In situations where the target motion is unknown, the HCRLB tends not to deviate far from the CRLB as the information about the target states is not very accurate compared to the large amount of data contributing to the biases.

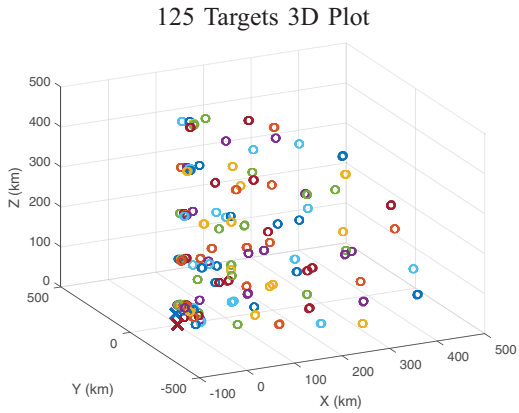

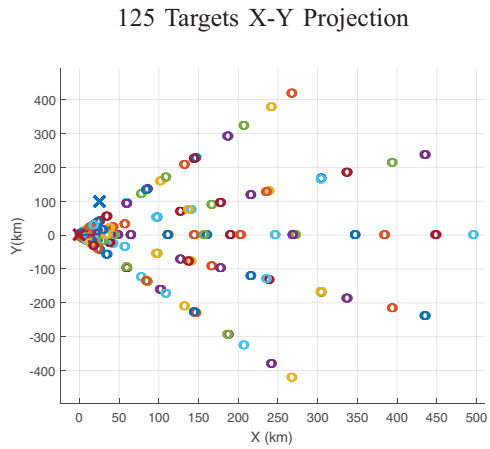

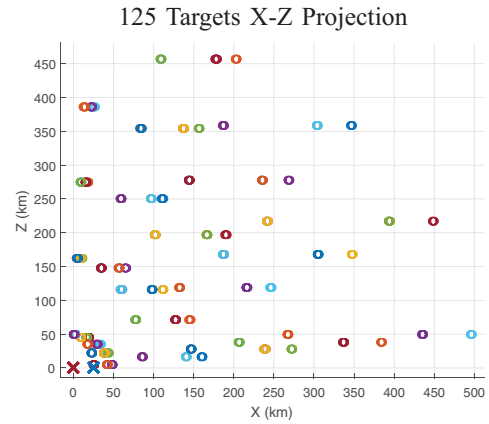

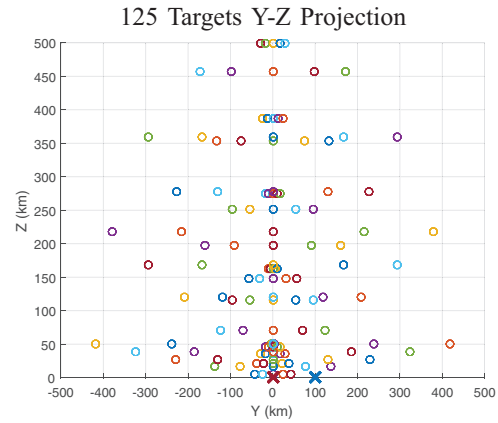

Figure 1. 125-target layout with projections. The × symbols represent sensors and the ○ symbols represent targets. (a) 3D plot. (b) X–Y projection. (c) X–Z projection. (d) Y–Z projection.

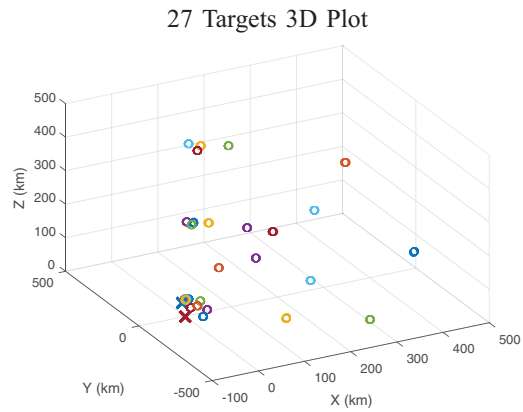

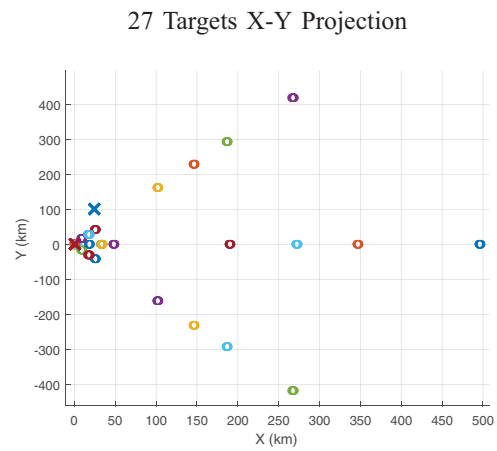

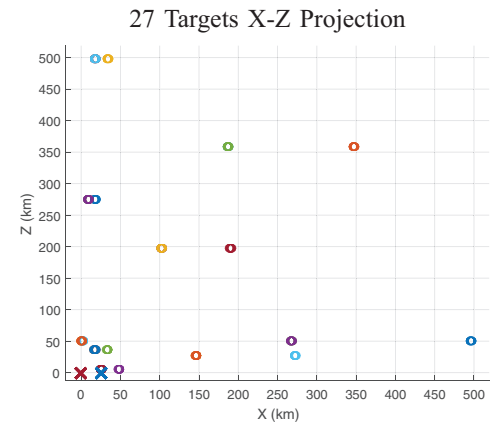

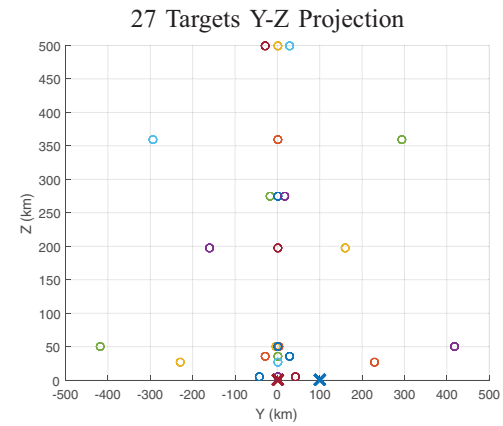

Figure 2. 27-target layout with projections. The × symbols represent sensors and the ○ symbols represent targets. (a) 3D plot. (b) X–Y projection. (c) X–Z projection. (d) Y–Z projection.

IV SIMULATION RESULTS

Simulations are made to test the performance of the approach proposed. Estimation of the biases can be difficult as a number of distinct targets must be used in order to differentiate the effects of the multiplicative and additive biases. In our simulation, sensor 1 is fixed at (0,0,0) km, sensor 2 is fixed at (25,100,0) km, and target velocity is $(-300, 0, 0)$ m/s. The target positions are set up in a cone extended from sensor 1. The ranges are in [50, 500] km, the azimuths are in $[-1, 1]$ rad, and the elevations are in [0.1, 1.5] rad. The additive and multiplicative biases, as well as the noise variances, are in range $[20\ \text{m}, 10^{-4}, 100\ \text{m}^2]$, and in azimuth and elevation $[3\ \text{mrad}, 3 \times 10^{-3}, 1\ \text{mrad}^2]$.

The target positions include a swath of range, azimuth, and elevation that allows each bias to make its effect apparent versus the other. In order to ensure this, the targets are radially placed in a cone from one sensor. In cases of high range, azimuth, and elevation values, the multiplicative biases dominate, whereas in cases of low range, azimuth, and elevation values, the additive biases dominate. In our simulations, the targets move at 300 m/s across time steps with ten measurements at one measurement per second. The sensor configuration is shown in Fig. 1 for 125 targets and in Fig. 2 for 27 targets.

The results of the simulations include the CRLB, RMSE from n_{MC} Monte Carlo runs, and a probability interval around the CRLB for each bias. The probability interval is calculated for the 95% region using the bias error samples from the Monte Carlo runs. The 95% probability interval is calculated by the following equations where σ_{SE} is the standard deviation of the squared error from the n_{MC} Monte Carlo runs:

$$0.95 = P(a < \text{RMSE} < b) \tag{41}$$

$$a = \sqrt{\text{CRLB} - 1.96 \cdot \frac{\sigma_{\text{SE}}}{\sqrt{n_{\text{MC}}}}} \tag{42}$$

$$b = \sqrt{\text{CRLB} + 1.96 \cdot \frac{\sigma_{\text{SE}}}{\sqrt{n_{\text{MC}}}}}. \tag{43}$$

A. Baseline Simulations

The first simulations are a baseline test to determine the performance and efficiency of the estimator. To begin, a simulation was performed with $N_T = 125$ targets and $K = 10$ time steps, the results of which are shown in Table III. In this simulation, it is shown that it is possible to achieve RMSE values that are compatible to the CRLB. The CRLB and RMSE are based on the error in the final bias estimates. The RMSE lies within the 95% probability interval around the CRLB in all cases; thus, the estimator is proved to be efficient [3]. Furthermore, the CRLB values are compared to the true bias and the noise standard deviation. Table III also contains the results that show that the residual bias RMSE is consistently lower than the noise standard deviation. Furthermore, the error from RMSE is lower than the noise standard deviation for

TABLE I
$n_{\text{MC}} = 100$ Runs, $K = 10$ Time Steps, and $N_T = 125$ Targets

Component	CRLB square root	HCRLB square root	RMSE	95% Probability interval around CRLB	Noise standard deviation	Uncorrected bias
Sensor 1 range additive	4.96 m	4.96 m	4.7 m	[4.3, 5.5] m	10 m	20 m
Sensor 1 range multiplicative	4.21×10^{-5}	4.21×10^{-5}	3.88×10^{-5}	$[3.66 \times 10^{-5}, 4.63 \times 10^{-5}]$	10 m	10^{-4}
Sensor 1 azimuth additive	4.85×10^{-2} mrad	4.85×10^{-2} mrad	5.55×10^{-2} mrad	$[3.98 \times 10^{-2}, 5.45 \times 10^{-2}]$ mrad	1 mrad	3 mrad
Sensor 1 azimuth multiplicative	7.89×10^{-5}	7.89×10^{-5}	7.56×10^{-5}	$[6.81 \times 10^{-5}, 8.80 \times 10^{-5}]$	1 mrad	3×10^{-3}
Sensor 1 elevation additive	1.15×10^{-1} mrad	1.14×10^{-1} mrad	1.27×10^{-1} mrad	$[9.24 \times 10^{-2}, 1.33 \times 10^{-1}]$ mrad	1 mrad	3 mrad
Sensor 1 elevation multiplicative	9.42×10^{-5}	9.41×10^{-5}	9.82×10^{-5}	$[7.74 \times 10^{-5}, 1.08 \times 10^{-4}]$	1 mrad	3×10^{-3}
Sensor 2 range additive	5.67 m	5.67 m	5.4 m	[5.0, 6.2] m	10 m	20 m
Sensor 2 range multiplicative	4.43×10^{-5}	4.43×10^{-5}	4.33×10^{-5}	$[3.80 \times 10^{-5}, 4.92 \times 10^{-5}]$	10 m	10^{-4}
Sensor 2 azimuth additive	8.44×10^{-2} mrad	8.44×10^{-2} mrad	9.32×10^{-2} mrad	$[6.65 \times 10^{-2}, 9.83 \times 10^{-2}]$ mrad	1 mrad	3 mrad
Sensor 2 azimuth multiplicative	6.82×10^{-5}	6.82×10^{-5}	8.00×10^{-5}	$[5.33 \times 10^{-5}, 7.97 \times 10^{-5}]$	1 mrad	3×10^{-3}
Sensor 2 elevation additive	9.66×10^{-2} mrad	9.66×10^{-2} mrad	1.00×10^{-1} mrad	$[8.18 \times 10^{-2}, 1.10 \times 10^{-1}]$ mrad	1 mrad	3 mrad
Sensor 2 elevation multiplicative	9.58×10^{-5}	9.56×10^{-5}	9.65×10^{-5}	$[8.15 \times 10^{-5}\ 1.07 \times 10^{-4}]$	1 mrad	3×10^{-3}

TABLE II
$n_{\mathrm{MC}} = 100$ Runs, $K = 10$ Time Steps, and $N_T = 27$ Targets

Component	CRLB square root	HCRLB square root	RMSE	95% Probability interval around CRLB	Noise standard deviation	Uncorrected bias
Sensor 1 range additive	7.7 m	7.7 m	8.3 m	[6.5, 8.7] m	10 m	20 m
Sensor 1 range multiplicative	8.84×10^{-5}	8.84×10^{-5}	9.15×10^{-5}	$[7.59 \times 10^{-5}, 9.84 \times 10^{-5}]$	10 m	10^{-4}
Sensor 1 azimuth additive	1.12×10^{-1} mrad	1.12×10^{-1} mrad	1.05×10^{-1} mrad	$[9.65 \times 10^{-2}, 1.23 \times 10^{-1}]$ mrad	1 mrad	3 mrad
Sensor 1 azimuth multiplicative	1.81×10^{-4}	1.81×10^{-4}	1.73×10^{-4}	$[1.56 \times 10^{-4}, 2.02 \times 10^{-4}]$	1 mrad	3×10^{-3}
Sensor 1 elevation additive	2.28×10^{-1} mrad	2.28×10^{-1} mrad	2.19×10^{-1} mrad	$[1.93 \times 10^{-1}, 2.59 \times 10^{-1}]$ mrad	1 mrad	3 mrad
Sensor 1 elevation multiplicative	1.82×10^{-4}	1.81×10^{-4}	1.72×10^{-4}	$[1.49 \times 10^{-4}, 2.08 \times 10^{-4}]$	1 mrad	3×10^{-3}
Sensor 2 range additive	11.1 m	11.1 m	11.4 m	[9.5, 12.4] m	10 m	20 m
Sensor 2 range multiplicative	9.64×10^{-5}	9.63×10^{-5}	1.01×10^{-4}	$[8.21 \times 10^{-5}, 1.08 \times 10^{-4}]$	10 m	10^{-4}
Sensor 2 azimuth additive	2.00×10^{-1} mrad	2.00×10^{-1} mrad	2.03×10^{-1} mrad	$[1.70 \times 10^{-1}, 2.25 \times 10^{-1}]$ mrad	1 mrad	3 mrad
Sensor 2 azimuth multiplicative	1.53×10^{-4}	1.53×10^{-4}	1.47×10^{-4}	$[1.32 \times 10^{-4}, 1.71 \times 10^{-4}]$	1 mrad	3×10^{-3}
Sensor 2 elevation additive	1.76×10^{-1} mrad	1.76×10^{-1} mrad	1.77×10^{-1} mrad	$[1.52 \times 10^{-1}, 1.98 \times 10^{-1}]$ mrad	1 mrad	3 mrad
Sensor 2 elevation multiplicative	1.82×10^{-4}	1.82×10^{-4}	1.79×10^{-4}	$[1.56 \times 10^{-4}, 2.03 \times 10^{-4}]$	1 mrad	3×10^{-3}

TABLE III
$n_{\mathrm{MC}} = 100$ Runs, $K = 1$ Time Steps, and $N_T = 125$ Targets

Component	CRLB square root	HCRLB square root	RMSE	95% Probability interval around CRLB	Noise standard deviation	Uncorrected bias
Sensor 1 range additive	16.4 m	16.4 m	17.5 m	[13.3, 18.8] m	10 m	20 m
Sensor 1 range multiplicative	1.36×10^{-4}	1.36×10^{-4}	1.24×10^{-4}	$[1.16 \times 10^{-4}, 1.52 \times 10^{-4}]$	10 m	10^{-4}
Sensor 1 azimuth additive	1.53×10^{-1} mrad	1.53×10^{-1} mrad	1.59×10^{-1} mrad	$[1.25 \times 10^{-1}, 1.72 \times 10^{-1}]$ mrad	1 mrad	3 mrad
Sensor 1 azimuth multiplicative	2.53×10^{-4}	2.53×10^{-4}	2.32×10^{-4}	$[2.21 \times 10^{-4}, 2.80 \times 10^{-4}]$	1 mrad	3×10^{-3}
Sensor 1 elevation additive	3.66×10^{-1} mrad	3.65×10^{-1} mrad	3.61×10^{-1} mrad	$[3.13 \times 10^{-1}, 4.12 \times 10^{-1}]$ mrad	1 mrad	3 mrad
Sensor 1 elevation multiplicative	3.01×10^{-4}	3.01×10^{-4}	2.83×10^{-4}	$[2.65 \times 10^{-4}, 3.31 \times 10^{-4}]$	1 mrad	3×10^{-3}
Sensor 2 range additive	18.7 m	18.7 m	17.8 m	[16.1, 20.8] m	10 m	20 m
Sensor 2 range multiplicative	1.43×10^{-4}	1.43×10^{-4}	1.27×10^{-4}	$[1.24 \times 10^{-4}, 1.59 \times 10^{-4}]$	10 m	10^{-4}
Sensor 2 azimuth additive	2.68×10^{-1} mrad	2.68×10^{-1} mrad	2.83×10^{-1} mrad	$[2.19 \times 10^{-1}, 3.08 \times 10^{-1}]$ mrad	1 mrad	3 mrad
Sensor 2 azimuth multiplicative	2.19×10^{-4}	2.19×10^{-4}	2.28×10^{-4}	$[1.81 \times 10^{-4}, 2.50 \times 10^{-4}]$	1 mrad	3×10^{-3}
Sensor 2 elevation additive	3.09×10^{-1} mrad	3.09×10^{-1} mrad	3.02×10^{-1} mrad	$[2.68 \times 10^{-1}, 3.47 \times 10^{-1}]$ mrad	1 mrad	3 mrad
Sensor 2 elevation multiplicative	3.05×10^{-4}	3.05×10^{-4}	3.05×10^{-4}	$[2.59 \times 10^{-4}, 3.43 \times 10^{-4}]$	1 mrad	3×10^{-3}

all cases except range multiplicative bias at the larger ranges.

This initial simulation contains many targets; therefore, another simulation is made with 27 targets instead. The results are displayed in same manner as before in Table I. The results show that the performance is not reduced much more than the 125-target case. The estimator is still efficient and has error in the angle biases that is lower than the noise standard deviation and the full bias. The range biases are significantly worse, and

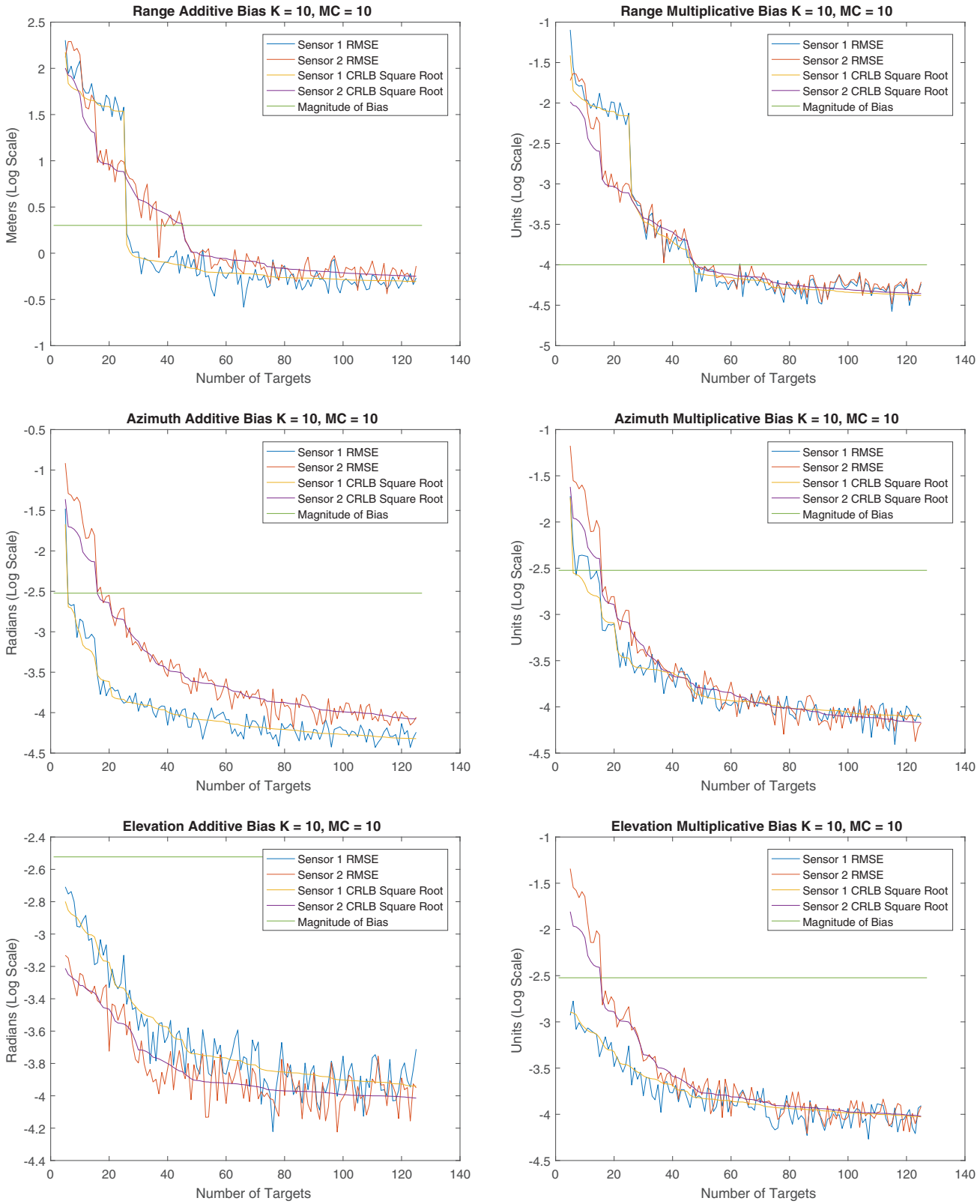

Figure 3. Comparing RMSE and CRLB with number of targets, $K = 10$ time steps.

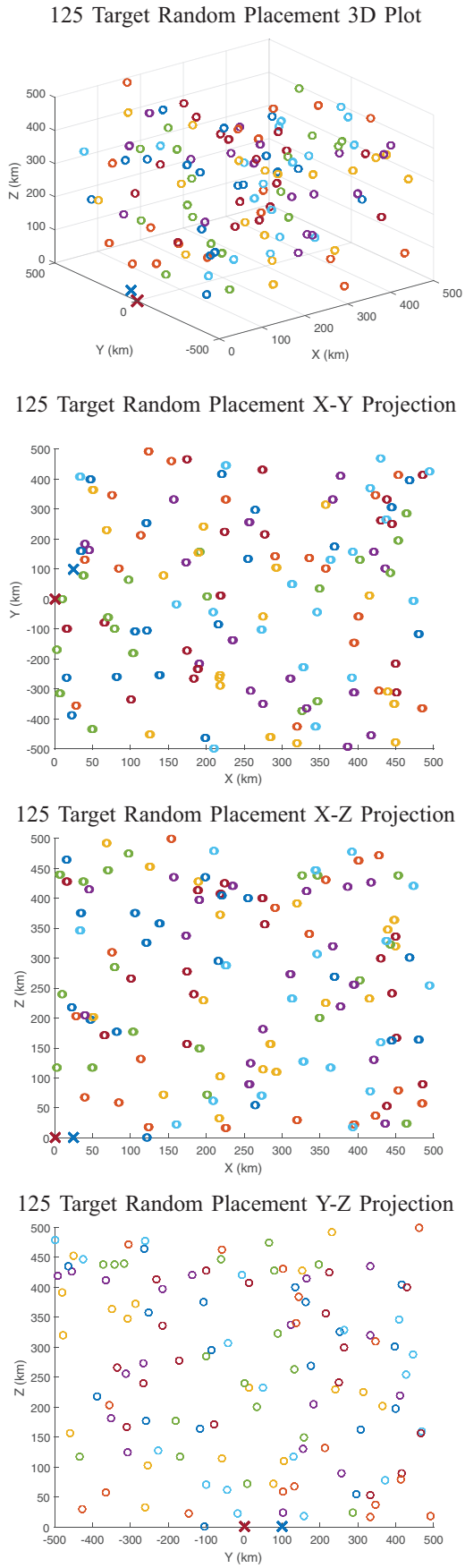

Figure 4. 125 random target layout with projections. The × symbols represent sensors and the ○ symbols represent targets. (a) 3D plot. (b) X–Y projection. (c) X–Z projection. (d) Y–Z projection.

the error in the range additive bias is almost equal to the noise standard deviation. The range multiplicative bias has RMSE that is nearly equal to the full bias, meaning that the estimation of this bias is comparable to not estimating it at all. Finally, a simulation is performed in which only a single measurement is available from each time step and with 125 targets. These results are provided in Table II. In this simulation, we see the results are very similar to the previous simulation with 10 time steps and 27 targets. The range bias estimates have RMSE that is poor and comparable to the full bias. The angle bias RMSE values are still lower than the noise standard deviation. The estimator is efficient although the CRLB itself is very poor for the range biases.

The HCRLB values for these simulations are nearly identical to the CRLB values, meaning that very little accuracy has been lost by using pseudo-measurements instead of the original measurements. This shows that when little information is known about the nuisance parameters, then the pseudo-measurement method is effective for avoiding the need to estimate the target state.

Efficient estimates are possible with this estimator and it is possible to reduce the CRLB to reasonable levels of variance by using measurements from many targets. In the case of only a single time step, the error is larger than the magnitude of the bias, meaning that it is necessary to include more measurements in order to achieve reasonable results. Furthermore, it is possible through bias estimation to reduce the error from the biases to levels that are less than the standard deviation of the noise, as shown in Tables I–III.

B. Comparing Performance Versus Number of Targets

Additionally, it is important to evaluate the bias estimation performance versus the number of targets. To simulate this, the number of targets is varied from 5 to 125 targets, starting with low-range targets and slowly expanding outward according to the target cone shown in Fig. 1. This means that range measurements have poor diversity and the estimates for the range biases are less accurate for small numbers of targets. The results of this simulation are given in Fig. 3. The results show that at around 45 targets the CRLB and RMSE are near the lowest point, and that further addition of targets continues to improve the results at a slow rate. Furthermore, we see that in the case of angle biases once there are 30 targets the bias RMSE values are about one-tenth of the full bias value. It is likely though that in a different target layout the results may differ, as this layout includes different combinations of range, azimuth, and elevation to ensure that the multiplicative biases can be estimated and not confused with the additive biases. To observe this difference, another simulation is made with random target placement.

In each Monte Carlo run, the targets are placed uniformly in a cube around the cone previously used. An example of this placement is given in Fig. 4. The same

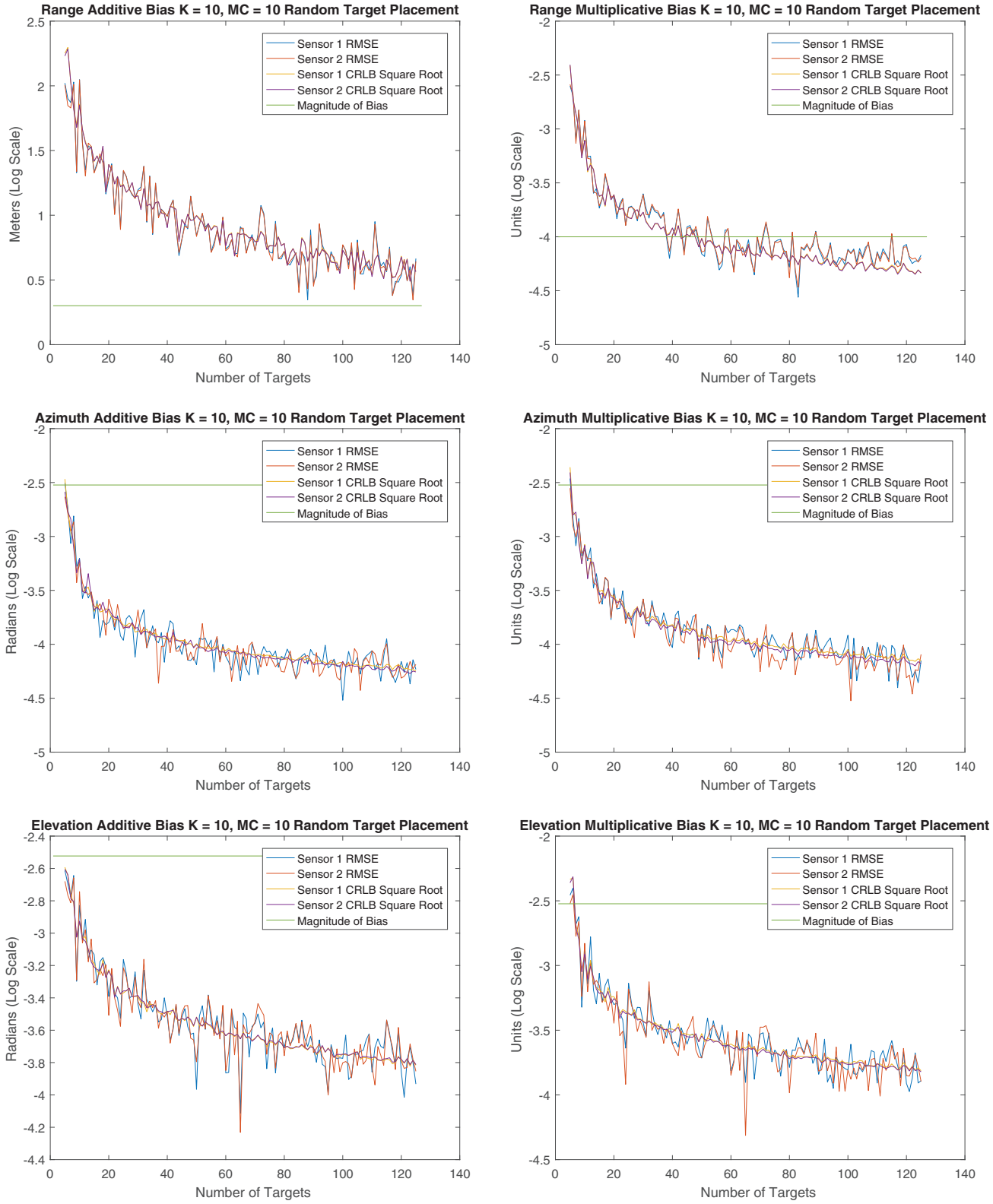

Figure 5. Comparing RMSE and CRLB with number of targets, $K = 10$ time steps.

simulation is made as earlier and the results are shown in Fig. 5. The results are nearly the same as before, except for the range additive bias. This is a result of the poor range diversity, especially of low-range targets. Overall, these results show that it is important to have measurement diversity to reduce the CRLB to reasonable levels and it is useful to have a large number of targets for this reason.

V. Conclusion

In this paper, an ML method is used to accurately estimate both multiplicative and additive biases in a

two-sensor scenario. Measurement data are converted into pseudo-measurements to isolate the effects of the biases in order to estimate them while ignoring estimation of the target state. The results show that despite the 12 separate estimated biases it is possible to match the RMSE and CRLB of the bias estimates by using a sufficient number of targets positioned in a manner to differentiate the biases. This proves the method is statistically efficient, although CRLB values are subject to the sensor and target geometry. In good conditions, the estimator can reduce the error from RMSE in bias estimates to a fraction of the noise standard deviation.

REFERENCES

[1] T. Asparouhov and B. Muthén
"Weighted least squares estimation with missing data,"
Mplus Technical Appendix, Jan. 2010.

[2] A. Balleri, A. Nehorai, and J. Wang
"Maximum likelihood estimation for compound-Gaussian clutter with inverse gamma texture,"
IEEE Trans. Aerosp. Electron. Syst., vol. 43, no. 2, PP. 775–779, Apr. 2007.

[3] Y. Bar-Shalom, X. R. Li, and T. Kirubarajan
Estimation With Applications to Tracking and Navigation: Theory, Algorithms and Software, New York: Wiley–Interscience, 2001.

[4] Y. Bar-Shalom, X. Tian, and P. Willett
Tracking and Data Fusion: A Handbook of Algorithms.
Storrs, CT: YBS Publishing, 2011.

[5] S. Fortunati, A. Farina, F. Gini, A. Graziano, M. S. Greco, and S. Giompapa
"Least squares estimation and Cramér–Rao type lower bounds for relative sensor registration process,"
IEEE Trans. Signal Process., vol. 59, no. 3, pp. 1075–1087, Mar. 2011.

[6] S. Fortunati, F. Gini, A. Farina, A. Graziano, M. S. Greco, and S. Giompapa
"On the application of the expectation–maximisation algorithm to the relative sensor registration problem,"
IET Radar, Sonar Navigation, vol. 7, no. 2, pp. 191–203, Feb. 2013.

[7] S. Fortunati, F. Gini, M. Greco, A. Farina, A. Graziano, and S. Giompapa
"An identifiability criterion in the presence of random nuisance parameters,"
in *Proc. 20th Eur. Signal Process. Conf.*, Aug. 2012, pp. 1194–1198.

[8] S. Fortunati, F. Gini, M. S. Greco, A. Farina, A. Graziano, and S. Giompapa
"An EM-based approach to the relative sensor registration in multi-target scenarios,"
in *Proc. IEEE Radar Conf.*, May 2012, pp. 602–607.

[9] S. Fortunati, F. Gini, M. S. Greco, A. Farina, A. Graziano, and S. Giompapa
"Least squares estimation and hybrid Cramér–Rao lower bound for absolute sensor registration,"
in *Proc. Tyrrhenian Workshop Adv. Radar Remote Sens.*, Sep. 2012, pp. 30–35.

[10] B. Friedland
"Treatment of bias in recursive filtering,"
IEEE Trans. Autom. Control, vol. 14, no. 4, pp. 359–367, Aug. 1969.

[11] D. Huang, H. Leung, and E. Bosse
"A pseudo-measurement approach to simultaneous registration and track fusion,"
IEEE Trans. Aerosp. Electron. Syst., vol. 48, no. 3, pp. 2315–2331, Jul. 2012.

[12] K. Kastella, B. Yeary, T. Zadra, R. Brouillard, and E. Frangione
"Bias modeling and estimation for GMTI applications,"
in *Proc. Int. Conf. Inf. Fusion*, Aug. 2000.

[13] M. Kowalski, D. Belfadel, Y. Bar-Shalom, and P. Willett
"CRLB for estimation of 3D sensor biases in spherical coordinates,"
Proc. SPIE Defense Secur.: Signal Process., Sensor/Inf. Fusion, and Target Recognit. XXVII, vol. 10646, no. 63, Apr. 2018.

[14] M. Levedahl
"Explicit pattern matching assignment algorithm,"
Proc. SPIE, vol. 4728, pp. 461–469, 2002. [Online]. Available: https://doi.org/10.1117/12.478526.

[15] X. Lin, Y. Bar-Shalom, and T. Kirubarajan
"Exact multisensor dynamic bias estimation with local tracks,"
IEEE Trans. Aerosp. Electron. Syst., vol. 40, no. 2, pp. 576–590, Apr. 2004.

[16] X. Lin, Y. Bar-Shalom, and T. Kirubarajan
"Multisensor–multitarget bias estimation of asynchronous sensors,"
Proc. SPIE, vol. 5429, pp. 105–116, 2004. [Online]. Available: https://doi.org/10.1117/12.542272.

[17] X. Lin, Y. Bar-Shalom, and T. Kirubarajan
"Multisensor multitarget bias estimation for general asynchronous sensors,"
IEEE Trans. Aerosp. Electron. Syst., vol. 41, no. 3, pp. 899–921, Jul. 2005.

[18] M. Longbin, S. Xiaoquan, Z. Yiyu, S. Z. Kang, and Y. Bar-Shalom
"Unbiased converted measurements for tracking,"
IEEE Trans. Aerosp. Electron. Syst., vol. 34, no. 3, pp. 1023–1027, Jul. 1998.

[19] N. N. Okello and S. Challa
"Joint sensor registration and track-to-track fusion for distributed trackers,"
IEEE Trans. Aerosp. Electron. Syst., vol. 40, no. 3, pp. 808–823, Jul. 2004.

[20] N. Okello and B. Ristic
"Maximum likelihood registration for multiple dissimilar sensors,"
IEEE Trans. Aerosp. Electron. Syst., vol. 39, no. 3, pp. 1074–1083, Aug. 2003.

[21] D. J. Papageorgiou and J. D. Sergi
"Simultaneous track-to-track association and bias removal using multistart local search,"
in *Proc. IEEE Aerosp. Conf.*, Mar. 2008.

[22] H. Rue and L. Held
Gaussian Markov Random Fields: Theory and Applications.
London, UK: Chapman & Hall/CRC, 2005.

[23] P. J. Shea, T. Zadra, D. Klamer, E. Frangione, R. Brouillard, and K. Kastella
"Precision tracking of ground targets,"
in *Proc. IEEE Aerosp. Conf. (Cat. No. 00TH8484)*, vol. 3, 2000, pp. 473–482.

[24] B. A. van Doorn and H. Blom
"Systematic error estimation in multisensor fusion systems,"
Proc. SPIE, vol. 1954, pp. 450–461, Oct. 1993.

Michael Kowalski received the B.S. degree in electrical engineering from the University of Connecticut, Storrs, CT, USA, in 2015. He is currently working toward the Ph.D. degree in electrical engineering at the Department of Electrical and Computer Engineering, University of Connecticut. His research interests include bias estimation as well as sensor fusion and target tracking.

Djedjiga Belfadel received the B.S. degree from the University of Mouloud Mammeri, Tizi Ouzou, Algeria, in 2003, the M.S. degree from the University of New Haven, West Haven, CT, USA, in 2008, and the Ph.D. degree from University of Connecticut, Storrs, CT, USA, in 2015, all in electrical engineering. She is currently an Assistant Professor with the Department of Electrical and Computer Engineering, Fairfield University, Fairfield, CT, USA. From 2009 to 2011, she was an Electrical Engineer with Evax Systems, Inc., Branford, CT, USA. Her research interests include target tracking, data association, sensor fusion, machine vision, and other aspects of estimation.

Yaakov Bar-Shalom (F'84) received the B.S. and M.S. degrees from the Technion, Haifa, Israel, in 1963 and 1967, respectively, and the Ph.D. degree from Princeton University, Princeton, NJ, USA, in 1970, all in electrical engineering. He is currently a Board of Trustees Distinguished Professor with the Department of Electrical and Computer Engineering and Marianne E. Klewin Professor with the University of Connecticut, Storrs, CT, USA. His current research interests include estimation theory, target tracking, and data fusion. He has authored or coauthored 600 papers and book chapters, and coauthored/edited 8 books, including *Tracking and Data Fusion* (YBS Publishing, 2011). He was elected Fellow of IEEE for contributions to the theory of stochastic systems and of multitarget tracking. He was an Associate Editor of the *IEEE Transactions on Automatic Control* and *Automatica*. He was General Chairman of the 1985 ACC, General Chairman of FUSION 2000, President of ISIF in 2000 and 2002, and Vice President for Publications during 2004–2013. Since 1995, he is a Distinguished Lecturer of the IEEE Aerospace and Electronic Systems Society. He was the corecipient of the M. Barry Carlton Award for the best paper in the *IEEE Transactions on Aerospace and Electronic Systems* in 1995 and 2000, and the recipient of the J. Mignona Data Fusion Award from the DoD JDL Data Fusion Group in 2002. He is a member of the Connecticut Academy of Science and Engineering. In 2008, he was the recipient of the IEEE Dennis J. Picard Medal for Radar Technologies and Applications, and in 2012 the Connecticut Medal of Technology. He was listed by academic.research.microsoft (top authors in engineering) as #1 among the researchers in aerospace engineering based on the citations of his work. He was the recipient of the 2015 ISIF Award for a Lifetime of Excellence in Information Fusion. This award was renamed in 2016 as the Yaakov Bar-Shalom Award for a Lifetime of Excellence in Information Fusion. He has the following Wikipedia page: https://en.wikipedia.org/wiki/Yaakov Bar-Shalom

Peter Willett received the B.A.S. degree in engineering science from the University of Toronto, Toronto, Ontario, Canada, in 1982, and the M.E., M.Sc., and Ph.D. degrees in electrical engineering from Princeton University, Princeton, NJ, USA, in 1983, 1984, and 1986, respectively. He is a faculty member with the Department of Electrical and Computer Engineering, University of Connecticut, Storrs, CT, USA, since 1986. Since 1998, he has been a Professor, and since 2003 an IEEE Fellow. His primary areas of research include statistical signal processing, detection, machine learning, communications, data fusion, and tracking. He is Chief Editor of *IEEE Aerospace and Electronic Systems Magazine* (2018–2020). He was Editor-in-Chief of *IEEE Signal Processing Letters* (2014–2016) and *IEEE Transactions on Aerospace and Electronic Systems* (2006–2011). He was also AESS Vice President for Publications (2012–2014). He is a member of the IEEE Fellows Committee, Ethics Committee, and Periodicals Committee, as well as the IEEE Signal Processing Society's Technical Activities and Conference Boards. He is also a member of the IEEE AESS Board of Governors and was Chair of IEEE Signal Processing Society's Sensor-Array and Multichannel Technical Committee.